IEEE Access
Multidisciplinary | Rapid Review | Open Access Journal

Received 29 September 2022, accepted 25 October 2022, date of publication 28 October 2022, date of current version 4 November 2022.

Digital Object Identifier 10.1109/ACCESS.2022.3218103

RESEARCH ARTICLE

Ultra-Low Crosstalk En/Decoder Using an Amplitude-Shaping Technique for 100 Gbps/λ OCDM-PAM-4 Transmission in O-Band

RACHATA MANEEKUT AND PASU KAEWPLUNG
Department of Electrical Engineering, Faculty of Engineering, Chulalongkorn University, Bangkok 10330, Thailand
Corresponding author: Pasu Kaewplung (pasu.k@chula.ac.th)

This work was supported by the Chulalongkorn University through the Second Century Fund (C2F).

ABSTRACT This paper proposes an optimized 16-chip multi-level phase-shifted optical code division multiplexing (OCDM) en/decoder for 4-level pulse amplitude modulation (PAM-4) format by using an amplitude-shaping (AS) technique. The optimized en/decoder can efficiently suppress the crosstalk and the primary beat noise (PBN). The code detection performance for 4-OCDM PAM-4 becomes the lowest to our knowledge. The numerical bit error rate analysis and the back-to-back simulation are shown. We also successfully demonstrate by computer simulation a 100 Gbps/λ enabling by 12.5 Gbaud 4-OCDM PAM-4 transmission in O-band over 6 × 30 km with in-line optical amplifiers.

INDEX TERMS Amplitude shaping, optical amplifier, o-band transmission, optical code division multiplexing, pulse amplitude modulation.

I. INTRODUCTION

Nowadays, the enormous growth in multimedia services such as 4K/8K video/game streaming, tele-working/medical services, cloud computing, blockchain technologies, and Metaverse based virtual/augmented reality (VR/AR) applications are key factors that are increasing the demand for data transmission in data center interconnects (DCI) rapidly [1], [2], [3], [4], [5]. Over the short distances of metro-DCI, ranges less than hundred kilometers, an intensity-modulation/direct-detection (IM/DD) system in O-band is commonly used due to its low cost, low complexity, and low chromatic dispersion (CD) [1], [6]. Various advanced modulation formats are implemented such as discrete multi-tone (DMT) [7], carrierless amplitude/phase modulation (CAP) [8] and M-level pulse amplitude modulation (PAM-M) [9], [10], [11]. Among these, the 4-level PAM (PAM-4) is one of the most promising candidates due to its low system complexity. It has already standardized in IEEE802.3bs for a 25 Gbaud PAM-4 signaling per wavelength over 10 km of a standard single-mode fiber (SMF) [12]. The extended reach version greater than 10 km has been standardized in IEEE802.3cn [13].

The associate editor coordinating the review of this manuscript and approving it for publication was Jiang Wu.

Although O-band has a zero-dispersion window, an inter-symbol interference (ISI) caused by CD can be a critical issue limiting the transmission reach and system baud rate because an electronic dispersion compensation (EDC) typically used in an optical coherent system cannot be used in IM/DD [19]. The dispersion in C-band could be managed by concatenating negative/positive dispersion fibers instead of using an EDC [15]. However, since the material dispersion is dominant, such dispersion managed fibers do not exist in O-band. To cope with ISI, other linear/nonlinear impairments, a feed-forward equalizer (FFE), and a decision-feedback equalizer (DFE) are candidates for sophisticated digital signal processing (DSP) algorithms for the IM/DD system, especially in O-band [14], [15], [16], [17].

To achieve a transmission rate of 100 Gbps per wavelength or beyond, two general approaches are to increase the modulation order and the transmission baud rate [6], [18], [19], [20]. Although the increase in modulation format to high-order PAM can utilize the existing optical bandwidth and optical transceivers more efficiently, it comes at a cost of higher system complexity and DSP. Furthermore, high-order PAM reduces eye height smaller than the lower-order PAM. In the sense of signal detection, high-order PAM requires higher signal-to-noise ratio (SNR) to

let receivers distinguish them. Conversely, to increase the baud rate, ultra-high speed opto-electronic transceivers as well as related electronic devices are needed to be upgraded. Moreover, high baud rate PAM experiences massive attenuation in high-frequency signal components, which need powerful DSP and advanced coding techniques to deal with this impairment [17]. Although a multi-source agreement (MSA) has recently announced a technical specification of 400GBASE-LR4-10, which can support 4 coarse wavelength division multiplexing (CWDM) channels employing PAM-4 signaling at 53 Gbaud, the operating distance is limited to only 10 km [21]. Therefore, the system migration to a transmission rate of 100 Gbps/wavelength with a longer distance whilst keeping the baud rate low is a challenging target.

Optical code-division multiplexing (OCDM) is another dimension for signal multiplexing beyond time/wavelength; therefore, we can transmit signals from many users employing the same optical spectrum simultaneously [22], [23], [24], [25], [26], [27], [28]. The signal of each user is en/decoded by optical en/decoders (E/D) without using any high chip-rate electronic devices. For example, a multi-port E/D-based array waveguide grating (AWG) [23], [24], and a superstructure fiber Bragg grating (SSFBG) with multi-level phase-shifted codes, or phase-shift-keying (PSK) codes [25] are key components in a coherent time-spreading (TS) OCDM system that can suppress the crosstalk from interfering spectral components with the superior performance to other codes. Consequently, the primary beat noise (PBN), which is the most dominant OCDM noise, decreases [24]. Previously, experimental work successfully demonstrated over a passive optical network (PON) with total bit rate of 160 Gbps [24], [26]. From these results, OCDM has shown the promising capability to increase the capacity of PAM-4 system.

Recently, the work in [27] has already shown the first demonstration of 10 Gbaud 4-OCDM PAM-3/PAM-4 over 20 km transmission in C-band. PAM-4 back-to-back bit error rate (BER) after the equalization reaches 2.4×10^{-2} at the received optical power (ROP) of -6 dBm. Nevertheless, the achievement in fiber transmission after 20 km has not been reported yet, but it reveals that crosstalk suppression by E/D is inadequate for PAM-4, although the 16-chip multi-port E/D has excellent performance for on-off-keying (OOK) format [24], [27]. Therefore, the enhancement in the crosstalk suppression is one of the most significant OCDM research topics. Researchers in [24], [26], and [28] have proposed many techniques to reduce the crosstalk. For example, the work in [24] has added 2 additional cascaded AWG E/D at the remote node (RN) whereas the work in [26] has added a quadrature phase-shift keying (QPSK) modulator and an additional AWG E/D to enable hybrid electrical/optical multi-level quadrature amplitude modulation (QAM) code. Finally, the work in [28] has applied extremely narrow-band optical band-pass filters (ENB-OBPF) to all decode ports of E/D to eliminate undesired spectral bands. Although these studies have reported the results with good crosstalk suppression for OOK, adding such additional E/D and ENB-OBPF may increase cost and complexity of the system.

Moreover, neither the analysis nor the demonstration of OCDM over PAM-4 from those solutions have been reported yet.

A high fiber attenuation in O-band, compared to C-band, is another issue that limits the system reach. Hence, the optical amplifiers (OA) are vital elements to compensate fiber loss as well as device insertion loss [29], [30], [31], [32]. Besides, a semiconductor optical amplifier (SOA) provides photonic integrated circuits with less power consumption but the system may suffer from self/cross gain modulation that causes SOA not to be preferable for IM/DD [6], [29]. Therefore, a Bismuth-doped fiber amplifier (BDFA) is an attractive type of doped fiber amplifier for O-band due to its ultra-wide 6-dB amplification bandwidth over 80 nm [31]. Demonstrations of using BDFA as a booster/pre-amplifier to extend the reach of a 25 Gbaud Nyquist PAM-4 signal and 400GBASE-LR-4/8, have been successfully reported in [29], [31], and [32]. As a result, these studies also show the possibility of introducing a multi-span high-speed IM/DD system using OA as in-line amplifiers to increase the distance of DCI.

In this paper, we propose the optimal design of optical E/D for OCDM PAM-4 system for the first time to our knowledge. The output signal from E/D experiences the optimized amplitudes under a Gaussian profile provided by an amplitude shaping (AS) technique. Power contrast ratio (PCR) and total PCR are investigated. The performance of ultra-low crosstalk E/D compared to previous E/D is also reported. We also analyze the theoretical BER of 4-OCDM PAM-4 based on our proposed E/D, and validate the results by a computer simulation. Finally, we show the 100 Gbps/λ of 12.5 Gbaud 4-OCDM PAM-4 signal transmission over 6×30 km of SMF with the OA as in-line amplifiers. All 4 OCDM users after equalization can achieve BER under the 7% overhead (OH) of hard-decision forward-error-correction (HD-FEC) limit.

II. AMPLITUDE-SHAPING EN/DECODER FOR OCDM PAM-4 FORMAT

Since the number of constellation points is increased from 2 to 4 (from OOK to PAM-4), the eye-height is decreased by a factor of 3. Therefore, PAM-4 signal is more sensitive to noises compared to OOK. To upgrade OCDM system from OOK to PAM-4, the noise suppression between codes is very important. This section shows the principle of the OCDM E/D impulse and frequency response design. After that, we evaluate the code detection performance and show the effectiveness of the optimal design E/D, respectively.

A. PRINCIPLE OF TIME-SPREADING AS-OCDM EN/DECODER

In the coherent TS-OCDM system, a series of N optical pulses are obtained as an encoded signal after a single ultra-short optical pulse is launched into the N-chip encoder

with chip period of t_{chip}. The total encoding period equals $N{\cdot}t_{\text{chip}}$ and we define a ratio of encoding period over bit period T_b as a spreading-time to bit period ratio (SBR). In this paper, SBR is 0.8, which is adequate to avoid ISI from a target user itself. The general expression of the output amplitude g at each chip number k of the encoded signal governed by the E/D is

$$g(k) = a \cdot \exp\left[-\frac{(k-b)^2}{2w^2}\right], \tag{1}$$

where a is corresponding to the highest peak of the encoded signal, b is the center position of the encoded signal which equals to $N/2$, and w is the Gaussian root-mean-square (RMS) width [33], [34]. As the ratio of b/w converges to zero, all N chips have equal amplitudes of a. This is the general scenario for most OCDM E/Ds, which we will call conventional OCDM E/Ds hereafter. On the contrary, the encoded signal will behave under a bell-shape Gaussian profile as the ratio b/w is slightly increased, and finally it will converge to all zero amplitudes as the b/w tends to infinite. By combining the amplitude function $g(k)$ with the impulse response of the conventional E/D based multi-level PSK codes, the impulse response under the Gaussian shaping profile is [35],

$$h_{\text{code}-c}(t) = \sum_{k=0}^{N-1} \sqrt{g(k+1)} \times \exp\left[-\text{j}\frac{2\pi k}{N}(c-1)\right] \cdot\delta\left(t - k\frac{T_b \cdot \text{SBR}}{N}\right), \tag{2}$$

where, c is the code number. Then, the frequency response of the E/D is

$$H_{\text{code}-c}(f) = \sum_{k=0}^{N-1} \sqrt{g(k+1)} \times\exp\left[-\text{j}2\pi k\left(\left(\frac{c-1}{N}\right) + f\frac{T_b \cdot \text{SBR}}{N}\right)\right]. \tag{3}$$

As a result, after the encoder, the optical field of the encoded signal can be expressed as

$$E_{\text{code}-c}(t) = \sum_{k=0}^{N-1} \sqrt{g(k+1)} \times \exp\left[-\text{j}\frac{2\pi k}{N}(c-1)\right] \times\exp\left[-\frac{\left(t - k\left(T_b \cdot \text{SBR}/N\right)\right)^2}{2T_0^2}\right]. \tag{4}$$

At the decoder, the encoded signal from (4) will be decoded by a decoder. The correlation between impulse response in (2) and encoded signal in (4) returns a decoded signal. As the phase-shifted sequences or codes inside encoders and decoders are matched, the decoders return $E_{\text{acp}}(t)$ with high amplitudes called auto-correlation peak (ACP). On the other hand, in a case that the code does not match, the incorrectly decoded signals $E_{\text{ccp}}(t)$ called cross-correlation peaks (CCP) are generated with low amplitudes compared to ACP instead.

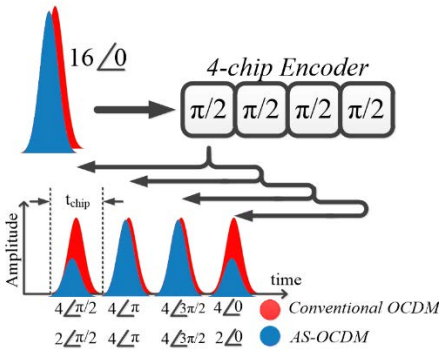

FIGURE 1. Optical encoding process based SSFBG.

The graphical illustration of the conventional/AS-OCDM encoders based SSFBG depicts in Fig. 1. For example, in a case that the encoded signal with an amplitude {0.5, 1, 1, 0.5} is needed where {1} corresponds to the highest amplitude, the reflectivity of the 1st and the 4th chips of the AS-OCDM encoder should be designed to attenuate the amplitude of the reflected pulses by half.

Fig. 2 shows the decoding process. All 4 chips of encoded signal are launched into the decoder, resulting in various combinations of decoded pulses as a function of time. Note that the number of amplitudes and intensities in brackets correspond to AS-OCDM. The ACP is illustrated in the left side of Fig. 2 with the triangular-like shape in the conventional case whereas AS-OCDM exhibits a smoother shape than the conventional one with lower intensity. As the phase-shifted sequence does not match, the decoder returns CCP with very low amplitudes, as shown in the right side of Fig. 2. For conventional OCDM, the CCP amplitudes are {1, 0, 1, 0, 1, 0, 1}, and are {0.25, 0, 0, 0, 0,0, 0.25} for AS-OCDM, respectively. Note that the shape of CCP depends on the code distance between encoders and decoders.

B. TOTAL POWER CONTRAST RATIO AND THE OPTIMAL DESIGN OF EN/DECODER WITH ULTRA-LOW CROSSTALK

The PCR is generally used as the metric to measure the code detection performance of OCDM system employing the PSK code. PCR can be calculated from [24]

$$\text{PCR}(j) = 10\log\left(\frac{P_{\text{ccp}-i,j}}{P_{\text{acp}}}\right), \tag{5}$$

where P_{acp} and P_{ccp} are the average power of ACP and CCP which we can calculate by using (3) in [24]. Index i is the interfering user number that employs code #j in the code cardinality set. For example, in Fig. 2, the P_{acp} of conventional and AS-OCDM are 6.29 and 2.5 whereas the P_{ccp} of them are 0.57 and 0.018, respectively. Therefore, PCR for conventional and AS-OCDM are −10.42 and −21.42 dB, respectively. From this viewpoint, using AS-OCDM E/D can improve the code detection performance by 10 dB.

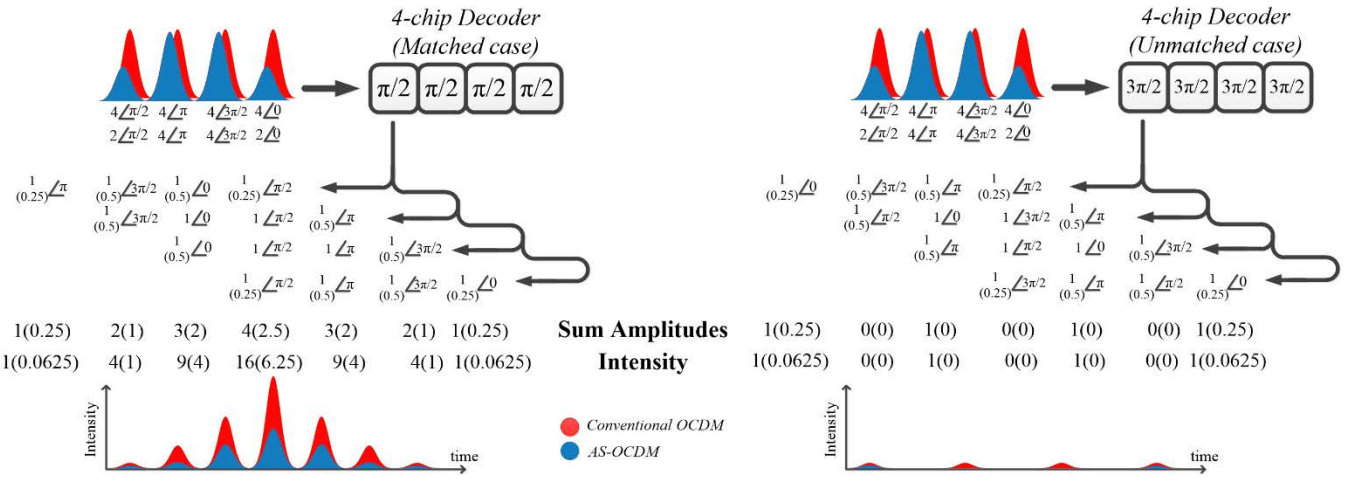

FIGURE 2. Schematic of decoding process based SSFBG for conventional and AS-OCDM.

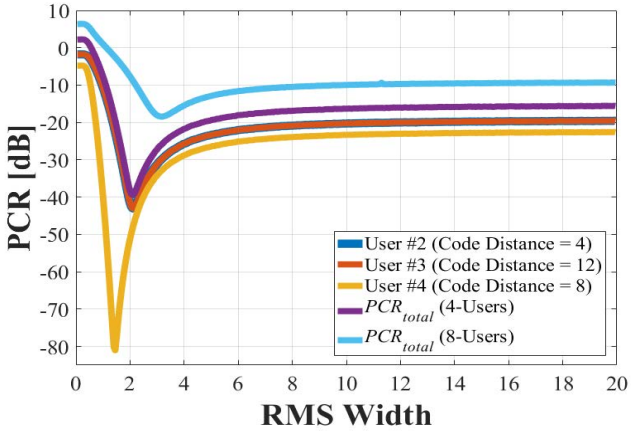

FIGURE 3. PCR and PCR total as a function of RMS width.

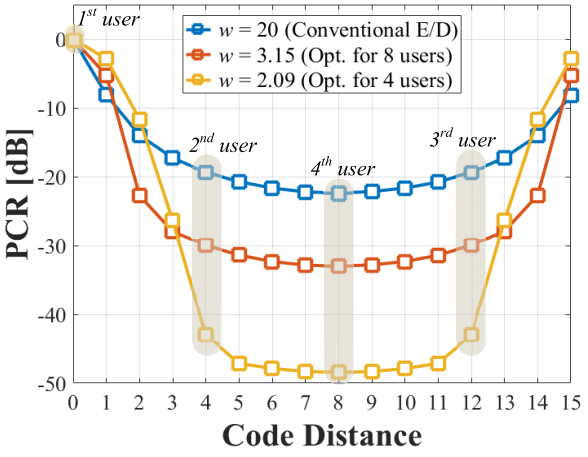

FIGURE 4. Relationship between code distance and PCR of E/D.

Nevertheless, PCR just measures between the target user and each single interfering user only. In a multi-user case, it is better to know the overall code detection performance in one metric. In this paper, we use the total PCR to characterize the AS-OCDM E/D. Total PCR is defined as [35]

$$\mathrm{PCR_{total}} = 10\log\left(\frac{\sum_{i=1}^{m} P_{\mathrm{ccp}-i,j}}{P_{\mathrm{acp}}}\right), \tag{6}$$

where m is the total number of interfering users.

We investigate the $\mathrm{PCR_{total}}$ of 4 OCDM PAM-4 users ($m = 3$) using 16-chip E/D as a function of Gaussian RMS width w. All 4 codes used in this investigation are code #1, #5, #9, and #13, to ensure the code distance of each adjacent code equals 4. For 8 users ($m = 7$), code #3, #7, #11, and #15 are also added and the code distance of each adjacent code is reduced to 2. The PCR of each specific code distance and $\mathrm{PCR_{total}}$ are shown in Fig. 3. The optimal $\mathrm{PCR_{total}}$ of AS-OCDM (optimized for 4 users) is -39.28 dB at $w = 2.09$. As w increases, $\mathrm{PCR_{total}}$ increases and converges to -15.28 dB which belongs to the conventional OCDM. In this case, we enhance $\mathrm{PCR_{total}}$ by 24 dB. Moreover, the optimal $\mathrm{PCR_{total}}$ which is optimized for of 8 OOK users is -18.44 dB at $w = 3.15$ and $\mathrm{PCR_{total}}$ converges to -9.13 dB as w exceeds 10 [35]. The $\mathrm{PCR_{total}}$ is improved by just only 9.31 dB.

Fig. 4 shows the PCR obtained from 3 types of E/Ds. The Gaussian RMS widths w are 20, 3.15, and 2.09 for conventional OCDM, and AS-OCDM E/D (optimized for 8 and 4 users), as shown in yellow, blue, and red solid lines, respectively. It is clearly seen when code #5, #9, and #13 are used (code distances are 4, 8, and 12), the PCR of each code is drastically decreased below -40 dB. Optical waveforms corresponding to encoded signal, ACP, and CCP are also shown in Fig. 5. All waveforms in Fig. 5(a)-(b) are normalized to have the highest peak of 1.

The frequency response of the E/D for all 3 interested cases are shown in Fig. 6. By employing AS-OCDM, it is confirmed that crosstalk from interfering spectral components is reduced from -20.11 dB in Fig. 6(a) down to -31.16, and -47.54 dB as shown in Fig. 6(b)-(c), respectively. The

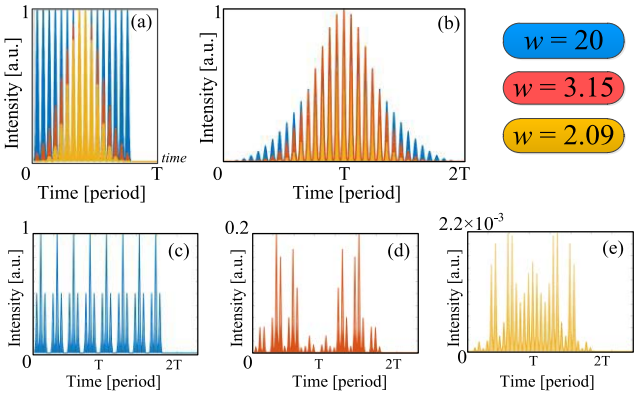

FIGURE 5. Optical waveforms from E/D (a) encoded signal, (b) ACP, CCP of 2 nd user from (c) w = 20, (d) w = 3.15, and (e) w = 2.09.

crosstalk in Fig. 6(c) is improved by 27.43 dB compared to Fig. 6(a).

As a result, regards PCR_{total}, PCR and E/D frequency response, we also can infer that AS-OCDM E/D with optimal w can improve the code orthogonality between the target and interfering users which will be able to effectively suppress PBN as well. The concept of shaping the encoded signal into a Gaussian-like shape, enabled by AS-OCDM E/D, has been demonstrated by another method called time-extended multi-level QAM-based optical codes [26]. Similar to this work, the encoded signal amplitudes in [26] exhibit a stair-step function in Gaussian-like shape instead of uniform amplitudes. The experimental results showed that PCR values and frequency response of the E/D had also improved.

III. NUMERICAL BER ANALYSIS AND OPTICAL BACK-TO-BACK SIMULATION

In this section, the performance evaluation of AS-OCDM PAM-4 E/D using BER will be described. Firstly, we numerically calculate the theoretical BER. Then, to verify our results, the computer simulation using MATLAB is performed to investigate the system in back-to-back cases.

A. THEORETICAL BER ANALYSIS

In the coherent TS-OCDM, the decision signal detected at the photodiode (PD) is,

$$Z = \Re \int_0^{T_b} E_{\text{acp}}(t) \cdot E^*_{\text{acp}}(t)\, dt + \Re \sum_{i=1}^{m} \int_0^{T_b} E_{\text{ccp}-i}(t) \cdot E^*_{\text{ccp}-i}(t)\, dt + 2\Re \sum_{i=1}^{m} \int_0^{T_b} E_{\text{acp}}(t) \cdot E^*_{\text{ccp}-i}(t)\, dt + 2\Re \sum_{j=i+1}^{m} \sum_{i+1}^{m-1} \int_0^{T_b} E_{\text{ccp}-\mathbf{i}}(t) \cdot E^*_{\text{ccp}-j}(\mathbf{t})\, dt + \int_0^{T_b} n_0(t)\, dt, \tag{7}$$

where $\Re$ is the PD responsivity [24]. The first term is the target signal. The second term is the MAI noise. The third term is the PBN noise. The fourth term is the secondary beat noise (SBN). The last term refers to Gaussian random noise at the receiver. For OCDM PAM-4 where all levels are equally spaced, the ROP at the PD represents the average power $P_d = P_{\text{acp}}(1 + PCR_{\text{total}})$. In this case, the relationship between P_d and the average power of level 3 is $P_3 = 2P_d$. Therefore, the average power of level 0-2 can be derived as a function of P_{d} and extinction ratio (ER) of the optical modulator as

$$P_0 = \frac{2P_{\text{d}}}{\text{ER}}, \tag{8}$$

$$P_1 = \frac{2P_{\text{d}}(\text{ER}+2)}{3\text{ER}}, \tag{9}$$

$$P_2 = \frac{2P_{\text{d}}(2\text{ER}+1)}{3\text{ER}}. \tag{10}$$

As a result, the average photocurrent at each level is

$$I_p = \Re P_p, \tag{11}$$

where index p is the PAM-4 amplitude level {0, 1, 2, 3}. The numerical BER is usually used to evaluate the system performance of OCDM PAM-4. Firstly, we start with the symbol error rate (SER) calculation for PAM-4 which is stated as [9]

$$\text{SER} = \frac{1}{8}\left[\text{erfc}\left(\frac{I_{\text{th}-01}-I_0}{\sqrt{2}\sigma_0}\right) + \text{erfc}\left(\frac{I_1-I_{\text{th}-01}}{\sqrt{2}\sigma_1}\right) + \text{erfc}\left(\frac{I_{\text{th}-12}-I_1}{\sqrt{2}\sigma_1}\right) + \text{erfc}\left(\frac{I_2-I_{\text{th}-12}}{\sqrt{2}\sigma_2}\right) + \text{erfc}\left(\frac{I_{\text{th}-23}-I_2}{\sqrt{2}\sigma_2}\right) + \text{erfc}\left(\frac{I_3-I_{\text{th}-23}}{\sqrt{2}\sigma_3}\right)\right]. \tag{12}$$

Note that I_0-I_3 and σ_0-σ_3 are average amplitudes and standard deviations of levels 0 to 3, $I_{\text{th}-01}$-$I_{\text{th}-23}$ are threshold amplitudes between each consecutive level. The noise variance for each level can be expressed as [36]

$$\sigma^2_{\text{total}-p} \approx \sigma^2_{\text{PBN}-p} + \sigma^2_{\text{rx}-p}. \tag{13}$$

The term $\sigma^2_{\text{PBN}-p}$ is the variance of PBN. It can be calculated from

$$\sigma^2_{\text{PBN}-p} = \frac{\Re^2}{\pi} \sum_{i=1}^{m} \int_0^{2\pi} \int_0^{T_b} E^2_{\text{acp}-p}(t) \cdot E^2_{\text{ccp}-i}(t) \cdot \cos^2\theta_j dt d\theta_j, \tag{14}$$

where $\theta_j = \emptyset_{\text{acp},p}(t) - \emptyset_{\text{ccp}-i}(t)$ is the phase difference between ACP and CCP considering a random process within $[-\pi, \pi]$ [24], [28]. The largest interfering effect where all m interfering users transmit the highest amplitude level simultaneously is assumed in this calculation. In (13), for simplification, we assume $\sigma^2_{\text{PBN}-0} = 0$ when the target user transmits

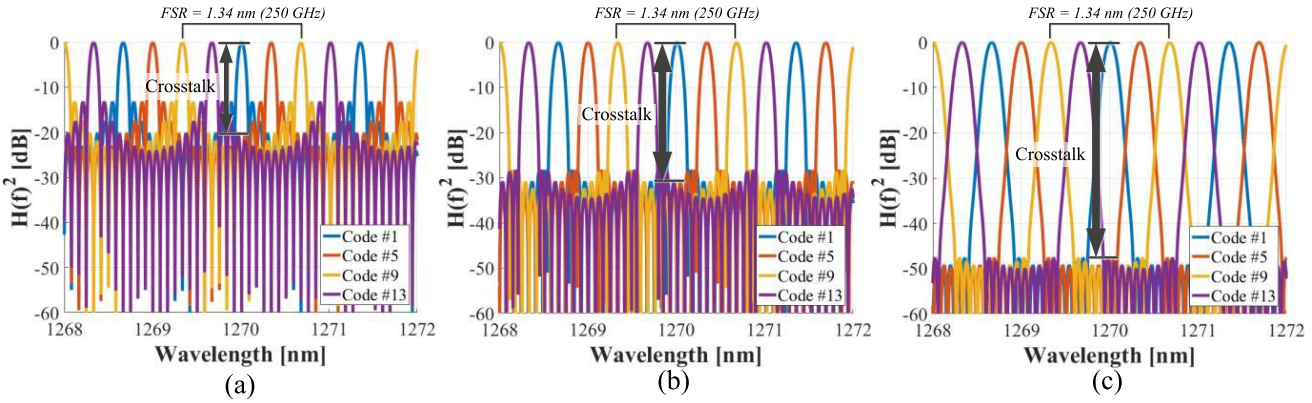

FIGURE 6. Optical spectra of OCDM E/D (a) conventional OCDM, (b) optimized for 8-users, and (c) optimized for 4-users.

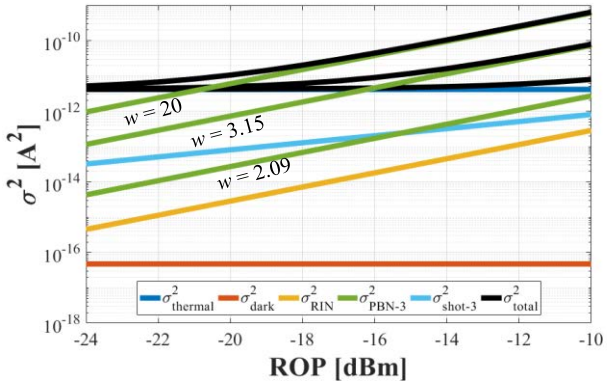

FIGURE 7. Noise contributions as a function ROP.

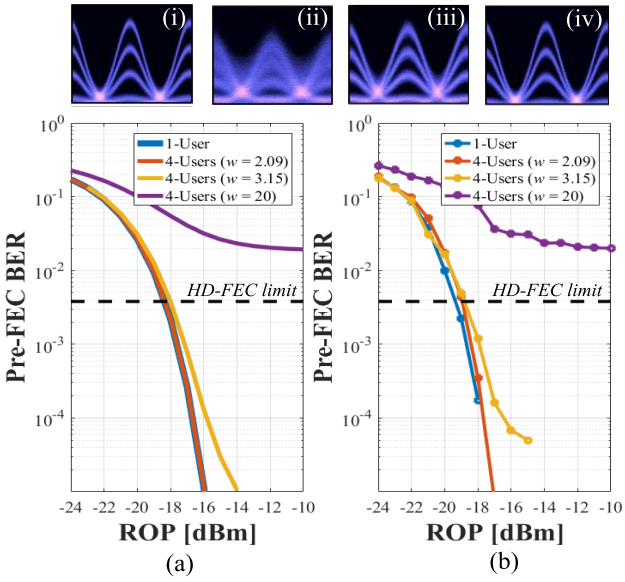

FIGURE 8. B-to-B performance as a function of ROP (a) numerical BER, and (b) simulation BER.

level $p = 0$. The second term in (13) is the total receiver noise $\sigma^2_{\mathrm{rx}-p}$, and is expressed as

$$\sigma^2_{\mathrm{rx}-p} = \frac{4k_B\Delta fT}{R_L} + 2qI_p\Delta f + 2qI_{\mathrm{d}}\Delta f + \mathrm{RIN}I_p^2\Delta f. \quad (15)$$

All 4 noise terms correspond to thermal noise, shot noise, dark current noise, and relative intensity noise (RIN), respectively. The parameters denoted by k_B, R_L, T, q, I_{d}, Δf, and RIN are Boltzmann constant, load resistance, temperature in Kelvin, electron charge, dark current, receiver bandwidth, and average RIN spectral density, respectively. Parameter values used for numerical calculation are $\Re = 0.85$ A/W, ER = 13 dB, $R_L = 50\Omega$, $T = 300$K, $I_{\mathrm{d}} = 10$nA, $\Delta f = 12.5$GHz, and RIN $= -145$ dB/Hz. Then, the threshold amplitudes among adjacent levels are optimized from

$$I_{\mathrm{th}-p,p+1} = \frac{(\sigma_{p+1}\cdot I_p + \sigma_p \cdot I_{p+1})}{(\sigma_p + \sigma_{p+1})}. \quad (16)$$

Finally, the BER can be approximated from

$$\mathrm{BER} = \frac{(d_{\mathrm{avg}} \times \mathrm{SER})}{\log_2 M} \quad (17)$$

where, d_{avg}, and M are average Hamming distance of each consecutive level and number of PAM levels which equal to 1 (for Gray coding) and 4, respectively.

All noise contributions in 4-OCDM PAM-4 are plotted in Fig. 7. All 4 codes are code #3, #7, #11, and #15. This code set still preserves the least code distance of 4 between each adjacent code. In conventional OCDM E/Ds with $w = 20$, the $\boldsymbol{\sigma}^2_{\mathrm{PBN}}$ dominates over other noises at ROP over -21 dBm. It is clearly shown in Fig. 7 that the optimized E/Ds can suppress $\boldsymbol{\sigma}^2_{\mathrm{PBN}}$. OCDM E/Ds with $w = 3.15$ and 2.09 can reduce $\boldsymbol{\sigma}^2_{\mathrm{PBN}}$ by 9.17, and 23.46 dB compared to the conventional case.

The numerical BER of 1-user and 4-user cases, calculated from (17), is shown in Fig. 8(a). Note that all noise terms that are generated from CCP become zero in 1-user case. For the 1-user case, the BER calculated from $w = 2.09$ achieve the HD-FEC limit at ROP $= -18.38$ dBm. For the 4-user case using conventional E/D, although $\mathrm{PCR}_{\mathrm{total}}$

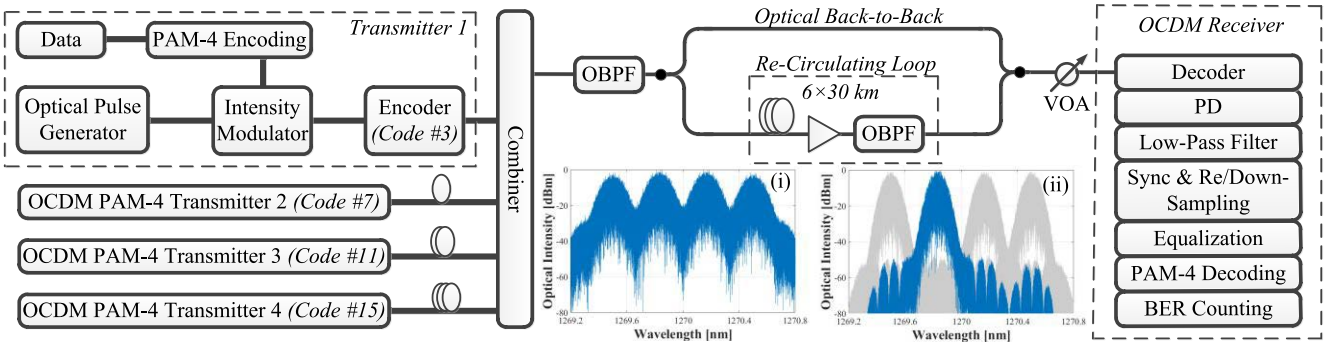

FIGURE 9. System architecture of OCDM PAM-4.

is −15.28 dB, which is improved by 6.15 dB compared to PCR_{total} of 8 OOK-user case, BER is not good enough to surpass HD-FEC limit as expected, and it reaches the error-floor at 2×10^{-2}. For $w = 3.15$, we achieve the HD-FEC limit at the ROP of −18 dBm. The power penalty caused by mainly σ^2_{PBN} is 0.38 dB. For $w = 2.09$, we successfully suppress σ^2_{PBN} and the numerical BER almost converges to the 1-user case. The power penalty in this case is approximately 0.01 dB.

B. OPTICAL BACK-TO-BACK SIMULATION

The simulation block diagram is shown in Fig. 9. The system baud rate is 12.5 Gbaud. The center wavelength of the optical source and E/Ds are 1270 nm. The optical pulse generator generates 2-ps of full-width half maximum (FWHM) pulses at a repetition rate of 12.5 GHz. For each user, the total 120000 random binary bits are modulated with an intensity modulator with ER = 13 dB to generate a 12.5 Gbaud PAM-4 signal employing Grey-coding. In this case, we use the equidistant PAM-4 where the space between each PAM level is uniform. PAM-4 signal is then encoded with programmable 16-chip encoders. All 4 codes are the same code set as codes already used in the numerical analysis. The encoder SBR is 0.8. Therefore, the total number of chips in one symbol duration is 20. The encoder has a chip period of 4 ps with the free spectral range (FSR) of 250 GHz. The sampling rate is 4 samples/chip which results in 80 samples/symbol. Before combining all signals together, the specific values of delays are applied to each interfering user to align the highest peaks of all 3 CCPs at the center of ACP. This delay adjustment guarantees the most severe interference in the asynchronous OCDM scenario. In the optical back-to-back, all 4 multiplexed signals are sent directly to the receiver side without considering the fiber recirculating loop. Inset (i) in Fig. 9 illustrates the simulated optical spectrum of all 4 encoded signals for the case of $w = 2.09$. In front of the decoder, the variable optical attenuator (VOA) is used to vary the ROP. Then, signals will be decoded by using the programmable 16-chip decoders. The decoded optical signal is detected at PD. The specifications of the PD are the same as numerical values. The detected signal is then processed by a simple DSP chain, including the low-pass filter (LPF), synchronization, down-sampling (to 1 sample/symbol), and PAM-4 decoding, respectively. Note that the received signal is synchronized with the reference transmitted signal by using cross-correlation function in MATLAB. In this case, no equalizations are performed. Finally, the BER is measured. The simulation results are shown in Fig. 8(b). For 1-user case, the BER achieves the HD-FEC limit at ROP = −19.35 dBm. The eye-diagram, obtained at −16 dBm, is very clear as shown in inset (i) of Fig. 8. In conventional E/Ds with 4 users, BER converges to 2×10^{-2} as ROP exceeds −12 dBm. The purple solid lines in Fig. 8(a) and 8(b) (numerical and simulation results) reach a good agreement with the experimental results shown in [27]. The eye-diagram in inset (ii) shows the severe interference, mainly from PBN. For the case of 4 users with optimized E/D at $w = 3.15$, the eye-diagram in inset (iii) reveals that the interference is significantly reduced. The receiver sensitivity of this case is at ROP = −18.81 dBm with the power penalty of 0.54 dB compared to the 1-user case. As the E/D is optimized at $w = 2.09$, we also obtain the eye-diagram in inset (iv) as clear as the 1-user case. The best receiver sensitivity in 4-users case can be achieved at ROP = −18.94 dBm with a power penalty of 0.41 dB. These results also confirm our numerical BER. With the optimal E/D design, the interference in a multi-user case can be eliminated and the BER characteristic is almost comparable to a single-user case. Therefore, we aim to break the previous OCDM PAM-4 limitations caused by the conventional E/Ds in the optical fiber transmission.

IV. O-BAND MULTI-SPAN FIBER SIMULATION WITH INLINE OPTICAL AMPLIFIERS

In section II and III, we show the crosstalk and PBN suppression with the optimal E/Ds design with an appropriate *w*. The graphical illustrations in Fig. 1 and 2 obviously show that adjusting the reflected amplitudes from E/Ds results in the shape of ACP and CCP. The ACP is attenuated but the CCP is considerably attenuated larger than the ACP, and this is the reason why PCR as well as PCR_{total} are improved. We also measure the ratio between P_{acp}, and the reference P_{acp} obtained from the conventional case, as a function of *w*. This ratio can be considered as the shaping loss due to the

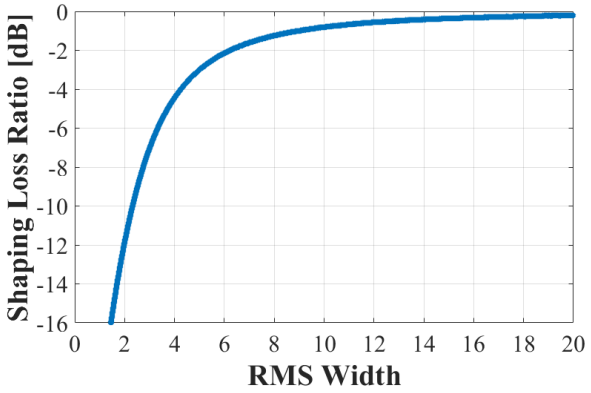

FIGURE 10. Relationship between shaping loss ratio and RMS width *w*.

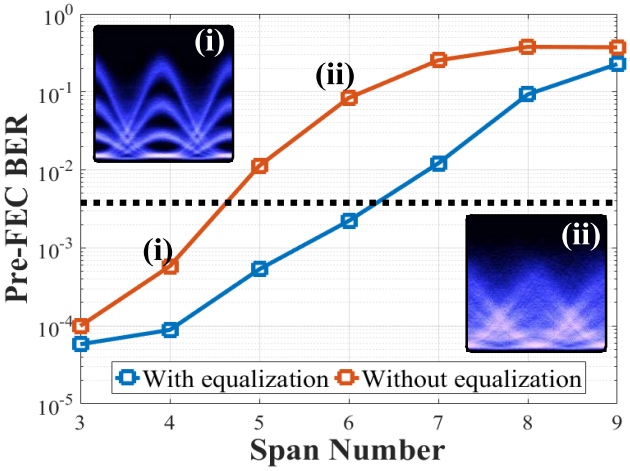

FIGURE 11. BER of each fiber span.

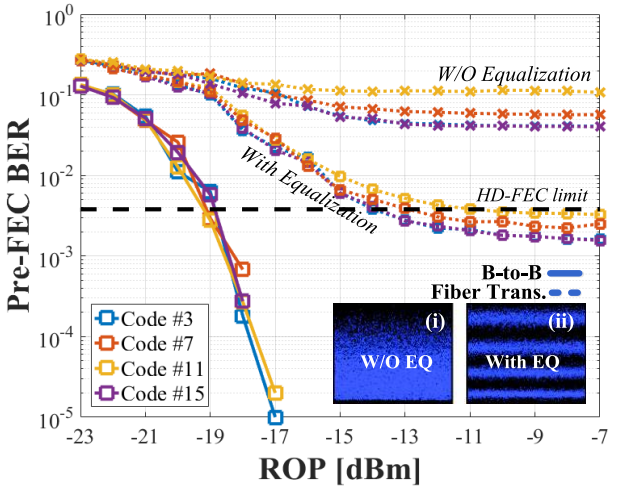

FIGURE 12. BER of back-to-back and 6 spans of fiber transmission.

AS approach and is shown in Fig. 10. At our optimal point at RMS width $w = 2.09$, the shaping loss is 11.31 dB. Although the shaping loss seems quite high, which can cause very low ROP in front of the PD, the ability of crosstalk-suppressed enhancement of 24 dB is preferable because the shaping loss and device insertion loss can be compensated by using the OA as a pre/booster amplifier. Moreover, placing the OA as in-line amplifiers along with a transmission fiber can enable a multi-span fiber transmission.

The system architecture of 4 users 12.5 Gbaud AS-OCDM PAM-4 ($w = 2.09$) multi-span transmission is already shown in Fig. 9. At the transmitter, the simulation parameters are the same as used in section III-B. The launched signal power into fiber is set to 8 dBm. At the fiber section, a re-circulating fiber loop, which consists of an SMF, an OA, and a 1.54 nm optical band-pass filter (OBPF), are added between the transmitters and the receivers. The SMF parameters used in the simulation have the attenuation and dispersion parameter of 0.5 dB/km and -4 ps/nm/km at 1270 nm. The fiber non-linear coefficient is 1.6 W^{-1}/km^{-1}. The fiber span length equals to 30 km with a total loss of 15 dB. The OA has the noise figure (NF) of 6 dB and the amplification gain of 15 dB at -7 dBm of input power. The gain reaches 17.5 dB for small input power below -20 dBm [32]. After the fiber transmission, the equalization, which consists of 11-taps T/2 spaced FFE, and 3-taps DFE with the least-mean square (LMS) algorithm, are added to the DSP chain at the receiver side to compensate ISI effects caused by CD. The equalized signal is used to optimize the transmitted PAM-4 level-spacing for each span separately [37].

Fig. 11 shows the average BER of the fiber transmission, as a function of the fiber span number. All BER is collected at $P_d = -7$dBm. At 4 spans of fiber, the eye-diagram of the decoded waveform at PD is shown in inset (i). The waveform is suffering from ISI. However, the eye-diagram is still clear enough that the signal decision can keep BER under the HD-FEC limit without using an equalization. The optimized PAM-4 level-spacing ratio from the base level to the top level is [0: 0.26: 0.60: 1]. On the other hand, the eye-diagram for 6 spans, with the optimized level-spacing of [0: 0.24: 0.58: 1] is shown in inset (ii) with a totally distorted waveform and the BER reaches 8.3×10^{-2}. After the equalization, the BER is improved to $2.2 \times 10^{-3}$and finally we can ensure the BER below the HD-FEC limit. Therefore, in a multi-span fiber transmission at the selected wavelength (1270 nm), CD is the dominant signal distortion that limits the distance.

The relationship between ROP and BER of back-to-back, and 6 spans of fiber-transmission is shown in Fig. 12. The back-to-back has a receiver sensitivity at ROP $= -18.94$ dBm. After fiber transmission, the decoded signal from code #3 is shown as a blue spectrum in inset (ii) of Fig. 9. Moreover, with total CD of -720 ps/nm, when the equalization is not applied, the pulse-broadening induced ISI is so severe that BER has the error-floor of around 0.04. On the other hand, the equalizers can enhance all received signals and BER successfully becomes lower than the HD-FEC limit with an error-floor of 1.56×10^{-3}. Decoded PAM-4 symbols without/with equalizations are illustrated as insets (i)-(ii) in Fig. 12, respectively. The receiver sensitivity is obtained at

ROP = −10.88 dB with the power penalty of 8.06 dB caused by the signal distortion in a fiber link compared back-to-back.

For further improvement in the reach extension, more powerful equalizations are needed to combat the largely accumulated CD. Another important issue is the development in OA to achieve higher gain with lower NF, respectively.

V. CONCLUSION

This paper proposed the ultra-low crosstalk 16-chip based PSK code OCDM E/D enabled by an AS technique to optimize the amplitudes of the E/D impulse response for arbitrary sets of total user number. The code detection performance including PCR and total PCR were used to obtain the optimal RMS width parameter for 4 AS-OCDM users employing PAM-4 data format. The total PCR of −39.28 dB, which was the lowest value to our knowledge for 4 OCDM users employing PAM-4 format, was reported. Theoretical BER was numerically analyzed and then it was verified by a computer simulation. Both results confirmed that the optimized AS-OCDM E/D for 4 users employing PAM-4 format was able to suppress crosstalk, and PBN in a multi-users case effectively. Therefore, these results showed a great opportunity to upgrade the modulation format to PAM-8. We aimed that this pilot design could act an encouragement to researchers for further research regarding E/D fabrications and implementations. Finally, we successfully transmitted by computer simulations a total bit rate of 100 Gbps/λ by using 12.5 Gbaud × 4-AS-OCDM PAM-4 over 6 × 30 km of SMF with in-line O-band OAs for DCI applications. All 4 users after the PAM-4 level-spacing optimization and equalizations could achieve the BER under 7% OH of HD-FEC limit with a power penalty of 8.06 dB.

REFERENCES

[1] C. Xie, "Optical interconnects in datacenters," in *Proc. Asia Commun. Photon. Conf.*, 2015.

[2] S.-M. Park and Y.-G. Kim, "A metaverse: Taxonomy, components, applications, and open challenges," *IEEE Access*, vol. 10, pp. 4209–4251, 2022, doi: 10.1109/ACCESS.2021.3140175.

[3] M. A. I. Mozumder, M. M. Sheeraz, A. Athar, S. Aich, and H.-C. Kim, "Overview: Technology roadmap of the future trend of metaverse based on IoT, blockchain, AI technique, and medical domain metaverse activity," in *Proc. 24th Int. Conf. Adv. Commun. Technol. (ICACT)*, Feb. 2022, pp. 256–261, doi: 10.23919/ICACT53585.2022.9728808.

[4] X. Pang, O. Ozolins, R. Lin, L. Zhang, A. Udalcovs, L. Xue, R. Schatz, U. Westergren, S. Xiao, W. Hu, G. Jacobsen, S. Popov, and J. Chen, "200 Gbps/lane IM/DD technologies for short reach optical interconnects," *J. Lightw. Technol.*, vol. 38, no. 2, pp. 492–503, Jan. 15, 2020, doi: 10.1109/JLT.2019.2962322.

[5] K. Zhong, X. Zhou, J. Huo, C. Yu, C. Lu, and A. P. T. Lau, "Digital signal processing for short-reach optical communications: A review of current technologies and future trends," *J. Lightw. Technol.*, vol. 36, no. 2, pp. 377–400, Jan. 15, 2018, doi: 10.1109/JLT.2018.2793881.

[6] K. Wang, J. Zhang, M. Zhao, W. Zhou, L. Zhao, and J. Yu, "High-speed PS-PAM8 transmission in a four-lane IM/DD system using SOA at O-band for 800G DCI," *IEEE Photon. Technol. Lett.*, vol. 32, no. 6, pp. 293–296, Mar. 15, 2020, doi: 10.1109/LPT.2020.2971648.

[7] W. Yan, L. Li, B. Liu, H. Chen, Z. Tao, T. Tanaka, T. Takahara, J. C. Rasmussen, and T. Drenski, "80 km IM-DD transmission for 100 Gbit/s per lane enabled by DMT and nonlinearity management," in *Proc. Opt. Fiber Commun. Conf.*, 2014, pp. 1–3.

[8] L. Tao, Y. Wang, Y. Gao, A. P. T. Lau, N. Chi, and C. Lu, "40 Gb/s CAP32 system with DD-LMS equalizer for short reach optical transmissions," *IEEE Photon. Technol. Lett.*, vol. 25, no. 23, pp. 2346–2349, Dec. 1, 2013.

[9] K. Szczerba, P. Westbergh, J. Karout, J. S. Gustavsson, A. Haglund, M. Karlsson, P. A. Andrekson, E. Agrell, and A. Larsson, "4-PAM for high-speed short-range optical communications," *IEEE/OSA J. Opt. Commun. Netw.*, vol. 4, no. 11, pp. 885–894, Nov. 2012.

[10] W. Wang, P. Zhao, Z. Zhang, H. Li, D. Zang, N. Zhu, and Y. Lu, "First demonstration of 112 Gb/s PAM-4 amplifier-free transmission over a record reach of 40km using 1.3 μm directly modulated laser," in *Proc. Opt. Fiber Commun. Conf.*, 2018, pp. Th4B–8.

[11] M. Yin, W. Wang, D. Zou, Q. Sui, X. Yi, Z. Li, and F. Li, "Low cost 100Gb/s/λ PAM-4 signal transmission for 40-km inter-DCI with 4-bit resolution DAC in O-band," in *Proc. Opt. Fiber Commun. Conf. (OFC)*, 2021, pp. 1–3.

[12] [Online]. Available: http://www.ieee802.org/3/bs/public

[13] *IEEE Standard for Ethernet—Amendment 4: Physical Layers and Management Parameters for 50Gb/s, 200Gb/s, and 400Gb/s Operation over Single-Mode Fiber*, IEEE Standard 802.3cn-2019 (Amendment to IEEE Standard 802.3-2018 as Amended by IEEE Standard 802.3cb-2018, IEEE Standard 802.3bt-2018, and IEEE Standard 802.3cd-2018), Dec. 2019, pp. 1–87, doi: 10.1109/IEEESTD.2019.8937109.

[14] D. Zou, F. Li, Z. Li, W. Wang, Q. Sui, Z. Cao, and Z. Li, "100G PAM-6 and PAM-8 signal transmission enabled by pre-chirping for 10-km intra-DCI utilizing MZM in C-band," *J. Lightw. Technol.*, vol. 38, no. 13, pp. 3445–3453, Jul. 1, 2020, doi: 10.1109/JLT.2020.2973902.

[15] N. Eiselt, J. Wei, H. Griesser, A. Dochhan, M. H. Eiselt, J.-P. Elbers, J. J. V. Olmos, and I. T. Monroy, "Evaluation of real-time 8 × 56.25 Gb/s (400G) PAM-4 for inter-data center application over 80 km of SSMF at 1550 nm," *J. Lightw. Technol.*, vol. 35, no. 4, pp. 955–962, Feb. 15, 2017, doi: 10.1109/JLT.2016.2617283.

[16] R. Nagarajan, I. Lyubomirsky, and O. Agazzi, "Low power DSP-based transceivers for data center optical fiber communications (invited tutorial)," *J. Lightw. Technol.*, vol. 39, no. 16, pp. 5221–5231, Aug. 15, 2021, doi: 10.1109/JLT.2021.3089901.

[17] T. Wettlin, S. Calabro, T. Rahman, J. Wei, N. Stojanovic, and S. Pachnicke, "DSP for high-speed short-reach IM/DD systems using PAM," *J. Lightw. Technol.*, vol. 38, no. 24, pp. 6771–6778, Dec. 15, 2020, doi: 10.1109/JLT.2020.3020649.

[18] Z. Liu, T. Xu, G. Saavedra, and P. Bayvel, "448-Gb/s PAM4 transmission over 300-km SMF-28 without dispersion compensation fiber," in *Proc. Opt. Fiber Commun. Conf.*, 2018, pp. 1–3.

[19] D. Che, Y. Matsui, R. Schatz, G. Raybon, V. Bhatt, M. Kwakernaak, and T. Sudo, "Long-term reliable >200-Gb/s directly modulated lasers with 800GbE-compliant DSP," in *Proc. Opt. Fiber Commun. Conf. (OFC)*, 2021, pp. 1–3.

[20] W. Wang, Z. Huang, B. Pan, H. Li, G. Li, J. Tang, and Y. Lu, "Demonstration of 214 Gbps per lane IM/DD PAM-4 transmission using O-band 35GHz-class EML with advanced MLSE and KP4-FEC," in *Proc. Opt. Fiber Commun. Conf. (OFC)*, 2020, pp. 1–3.

[21] [Online]. Available: http://100glambda.com/specifications/send/2-specifications/10-400g-lr4-10-technical-spec-rev1-0

[22] P. R. Prucnal, *Optical Code Division Multiple Access*, 1st ed. Boca Raton, FL, USA: CRC Press, 2005.

[23] G. Cincotti, N. Wada, and K. Kitayama, "Characterization of a full encoder/decoder in the AWG configuration for code-based photonic routers-Part I: Modeling and design," *J. Lightw. Technol.*, vol. 24, no. 1, pp. 103–112, Jan. 2006.

[24] T. Kodama, N. Wada, G. Cincotti, and K.-I. Kitayama, "Asynchronous OCDM-based 10 G-PON using cascaded multiport E/Ds to suppress MAI noise," *J. Lightw. Technol.*, vol. 31, no. 20, pp. 3258–3266, Oct. 15, 2013.

[25] R. Matsumoto, T. Kodama, S. Shimizu, R. Nomura, K. Omichi, N. Wada, and K. I. Kitayama, "40 G-OCDMA-PON system with an asymmetric structure using a single multi-port and sampled SSFBG encoder/decoders," *J. Lightw. Technol.*, vol. 32, no. 6, pp. 1132–1143, Mar. 15, 2014.

[26] T. Kodama and G. Cincotti, "Crosstalk-reduced OCDM system using time-extended multi-level QAM-based optical codes," in *Proc. Asia Commun. Photon. Conf. (ACP)*, Oct. 2018, pp. 1–3, doi: 10.1109/ACP.2018.8596005.

[27] T. Kodama, T. Miyazaki, M. Hanawa, A. Maruta, N. Wada, G. Cincotti, and K. Kitayama, "First demonstration of PAM4/PAM3-OCDM system for optical short-reach transmission," in *Proc. 23rd Opto-Electron. Commun. Conf. (OECC)*, Jul. 2018, pp. 1–2, doi: 10.1109/OECC.2018.8730023.

[28] T. Kodama, N. Wada, G. Cincotti, X. Wang, and K.-I. Kitayama, "Noise suppression using optimum filtering of OCs generated by a multiport encoder/decoder," *Opt. Exp.*, vol. 20, no. 9, pp. 10320–10329, Apr. 2012.
[29] Y. Hong, S. Deligiannidis, N. Taengnoi, K. R. H. Bottrill, N. K. Thipparapu, Y. Wang, J. K. Sahu, D. J. Richardson, C. Mesaritakis, A. Bogris, and P. Petropoulos, "ML-assisted equalization for 50-Gb/s/λ O-band CWDM transmission over 100-km SMF," *IEEE J. Sel. Topics Quantum Electron.*, vol. 28, no. 4, pp. 1–10, Jul. 2022, doi: 10.1109/JSTQE.2022.3155990.
[30] J. Zhang, W. Zhou, J. Xiao, J. Yu, M. Zhu, M. Lei, Y. Cai, Y. Zou, Q. Zhou, W. Xu, and J. Wang, "56 Gbit/s/λ PAM-4 IM/DD transmission over 120 km SSMF at O-band using cascaded semiconductor optical amplifiers for data center interconnects," in *Proc. Asia Commun. Photon. Conf./Int. Conf. Inf. Photon. Opt. Commun. (ACP/IPOC)*, 2020, pp. 1–3.
[31] V. Mikhailov, M. A. Melkumov, D. Inniss, A. M. Khegai, K. E. Riumkin, S. V. Firstov, F. V. Afanasiev, M. F. Yan, Y. Sun, J. Luo, G. S. Puc, S. D. Shenk, R. S. Windeler, P. S. Westbrook, R. L. Lingle, E. M. Dianov, and D. J. DiGiovanni, "Simple broadband bismuth doped fiber amplifier (BDFA) to extend O-band transmission reach and capacity," in *Proc. Opt. Fiber Commun. Conf. (OFC)*, 2019, pp. 1–3.
[32] Y. Wakayama, V. Mikhailov, D. J. Elson, R. Maneekut, J. Luo, C. Wang, F. Balasis, N. Yoshikane, D. Inniss, and T. Tsuritani, "400GBASE-LR4 transmission over field-deployed fibre link supported by bismuth-doped fibre amplifier," in *Proc. Eur. Conf. Opt. Commun. (ECOC)*, Sep. 2021, pp. 1–4.
[33] M. Mackenzie and K. Tieu, "Gaussian filters and filter synthesis using a Hermite/Laguerre neural network," *IEEE Trans. Neural Netw.*, vol. 15, no. 1, pp. 206–214, Jan. 2004.
[34] A. M. Kusters, M. Glade, and K. Heime, "Carrier lifetime measurement in semiconductor lasers using injection current pulses of Gaussian shape," *IEEE J. Quantum Electron.*, vol. 28, no. 12, pp. 2669–2673, Dec. 1992.
[35] R. Maneekut and P. Kaewplung, "Noise suppression using amplitude-shaping OCDM with 16-chip multi-level phase-shifted en/decoder," *IEEE Access*, vol. 6, pp. 50096–50104, 2018, doi: 10.1109/ACCESS.2018.2867940.
[36] T. Kodama, T. Miyazaki, M. Hanawa, A. Maruta, N. Wada, G. Cincotti, and K. Kitayama, "Demonstration of PAM4-OCDM system with electrical amplitude-level pre-tuning and post-equalization for data centers applications," *Opt. Exp.*, vol. 27, no. 8, pp. 11227–11235, 2019.
[37] J. Zhang, J. S. Wey, J. Shi, J. Yu, Z. Tu, B. Yang, W. Yang, Y. Guo, X. Huang, and Z. Ma, "Experimental demonstration of unequally spaced PAM-4 signal to improve receiver sensitivity for 50-Gbps PON with power-dependent noise distribution," in *Proc. Opt. Fiber Commun. Conf.*, 2018, pp. 1–3.

RACHATA MANEEKUT received the B.E., M.E., and Ph.D. degrees from the Microwave and Lightwave Communications Strategic Research Area, Department of Electrical Engineering, Faculty of Engineering, Chulalongkorn University, Thailand, in 2007, 2010, and 2018, respectively. From 2019 to 2021, he was a Research Engineer at the Photonic Transport Network and Photonics Innovation Laboratory, KDDI Research Inc., Japan. Since 2022, he has been a Researcher with the Department of Electrical Engineering, Faculty of Engineering, Chulalongkorn University. His research interests include the advance modulation scheme over optical access and short-reach networks, constellation shaping, and digital signal processing for optical transmission systems. In 2015, he received the Short-Term Research Fellowship from the National Institute of Information and Communications Technology (NICT), Japan. In 2017, he also received the Research Fellowship from the Photonic Transport Network Laboratory, KDDI Research Inc.

PASU KAEWPLUNG was born in Bangkok, Thailand, in December 1971. He received the B.S. and M.S. degrees in electrical engineering from Yokohama National University, Yokohama, Japan, in 1996 and 1998, respectively, and the Ph.D. degree in electrical engineering from Chulalongkorn University, in 2003. From April 1998 to March 2000, he conducted research at the Research Center for Advanced Science and Technology (RCAST), University of Tokyo, Japan. He is currently an Assistant Professor with the Microwave and Lightwave Communications Strategic Research Area, Department of Electrical Engineering, Faculty of Engineering, Chulalongkorn University. His research interests include optical access technology, optical fiber transmission systems, dispersion management, and the applications of nonlinear optical effects.